MARINE REPORTS 3(1) (2024) : 1-20
DOI: 10.5281/zenodo.12335495
marep@scopesscience.com

MARINE REPORTS
e-ISSN: 2822-5155
Journal homepage: https://scopesscience.com/index.php/marep/

*Received: 20 May 2024; Received in revised form: 04 June 2024*
*Accepted: 04 June 2024; Available online: 25 June 2024*
RESEARCH PAPER

**Citation:** Mahpeykar, O., Ashtari Larki, A., & Akbarinasab, M. (2024). Automatic detection of eddies and influence of warm eddy on sound propagation in the Persian Gulf. *Marine Reports*, *3*(1), 1-20. https://doi.org/10.5281/zenodo.12335495

# AUTOMATIC DETECTION OF EDDIES AND INFLUENCE OF WARM EDDY ON SOUND PROPAGATION IN THE PERSIAN GULF

**Omid MAHPEYKAR[1*], Amir ASHTARI LARKI[1], Mohammad AKBARINASAB[2]**

[1] *Department of Physical Oceanography, Faculty of Marine Science and Oceanography, Khorramshahr University of Marine Science and Technology, Khorramshahr, Iran*
[2] *Department of Physical Oceanography, Faculty of Marine Science and Oceanography, University of Mazandaran, Babolsar, Iran*

**Corresponding author: o.mahpeykar@kmsu.ac.ir, +989166404715, ORCID: 0000-0002-6592-3856*

## Abstract
Eddies are among the most complex phenomena in marine environments, with significant impacts on hydrodynamic parameters. Various intelligent algorithms are utilized to identify and analyze these eddies. In this study, a vector geometry algorithm based on the rotation of velocity vectors was employed to detect and extract eddies in the Persian Gulf. The algorithm utilizes horizontal velocity components from numerical modeling as inputs. Following eddy extraction, their characteristics were thoroughly examined. A total of 4308 cyclonic and 2860 anticyclonic eddies were identified at the surface, with 617 cyclonic and 329 anticyclonic eddies detected at a depth of 50 meters for daily data over one year. Additionally, an investigation into the impact of eddies on sound propagation revealed that warm eddies create areas of severe transmission loss at their centers, leading to divergence in sound rays.

**Keywords:** Persian Gulf, eddy, vector geometry algorithm, transmission loss (TL), acoustic

## Introduction
Eddies are comparatively large rotating water masses in the sea, resembling storms in the atmosphere, often accompanied by large ocean currents (Xiao et al., 2019). For instance, on the edges of the Kuroshio, there are often mesoscale eddies with a radius of tens to hundreds of kilometers. Eddies can form when the current becomes unstable, and this instability increases and makes the current to twist and finally produce an eddy (Fu et al., 2010). According to studies, eddies move gradually. Hence, compared to the dominant current, they can be thought of as a quasi-static structure in the water column (Zhang et al., 2014). Since hot or cold-water masses can be transported by eddies, characteristics such as temperature and salinity distribution of the basin noticeably alter. To the extent that these variations can influence the

concentration of nutrients, the diffusion of pollutants, and changes in the speed of sound in water (Li et al, 2011). Accordingly, the study of eddies is of great value in fishing, the environment, the military industry, and sailing. Methods of analyzing mesoscale eddies can result in their identification, observation, and tracking. Data that includes information about eddies involves remote sensing satellite data or the production of numerical models. It is impossible to examine the information of this data in the typical method, owing to its massive volume, spatially, and temporally (Dong et al., 2011). Hence, eddies are extracted and examined by automatic methods, which fall into four classes: Method of using physical parameters, methods of using wavelet analysis for relative vorticity field, methods of using geometric characteristics of streamlines, and method of using sea level anomaly characteristic (SLA). To use these methods, surface velocities and relative vorticity fields need to be available or determined. In this research, the method of geometric characteristics of streamlines was used to identify and extract eddies in the Persian Gulf. This research intended to identify and study eddies located in the Persian Gulf, based on the method of geometric characteristics of streamlines and using the products of the numerical model. The overall Persian Gulf circulation pattern is principally influenced by the prevailing northwesterly winds and the corresponding buoyancy fluxes and the corresponding momentums, then by heat-salinity forces and eventually by tidal forces (Thoppil & Hogan, 2010). Nevertheless, the details of this circulation are more complex than a cyclonic gyre, because seasonal changes in water exchange in the Strait of Hormuz, river inflows, wind intensity, and topographic anomalies, change it (Pous et al., 2015). In fact, this circulation consists of two scales:

1. Basin-scale: which is the general circulation and entails two currents: one to the northwest of the Strait of Hormuz along the Iranian coast in the northern part of the basin, and the other to Southeast in the southern part of the basin (Reynolds, 1993).
2. Mesoscale: which involves eddies with various dimensions that happen due to the existence of instability and the decomposition of the main rotation into a set of eddies. In summer, by reinforcing the stability of the water column and forming strong stratification, eddies form even with a diameter of more than 100 km. In late summer, these eddies alter the overall structure of the Persian Gulf to mesoscale ones. These conditions persevere in the basin for two to three months (Thoppil & Hogan, 2010).

The effect of the Eddies on sound propagation is important to oceanographers and submarine acoustics, especially since their understanding is widely used in the field of sound, submarine communications, and the obvious use of marine information. It is important to study how sound waves propagate in the marine environment in many industries, including shipbuilding, marine engineering, and military industries. Because measures such as depth measurement and depth mapping, voice communication and installation of sound arrays to identify subsurface targets are required to have a correct understanding of how sound waves propagate in the sea environment. Jia-xun et al. (2012) modeled mesoscale eddies and their effect on sound propagation under the sea. To this end, a theoretical computational model of oceanic mesoscale eddies based on hydrographic measurement data in the marine parts of the ocean was developed. The MMPE acoustic model was used to simulate the underwater sound propagation under the influence of eddies at different types, intensities and positions, at different frequencies and depths of the source. The results showed that warm-core eddy can make the convergence zone "move back" and the width of it increases, while cold-core eddy can make the convergence zone "move forward" and the width of it decreases. Xiao et al. (2019) investigated the effect of warm eddy on sound propagation in the Gulf of Mexico. First, the physical parameters of eddies, such as their lifetime, radius, and spatial distribution, were investigated using an automated method, and a strong warm eddy isolated from the Mexican stream was selected. Then, the effect of this strong warm eddy on sound propagation during its lifetime was

extensively analyzed by the parabolic equation and explained using normal mode and beam theory. The results showed that warm eddy can change the propagation path and cause the convergence region to be wider and closer to the sound source. In addition, warm eddy is able to dissipate sound energy, causing deep integrated energy to tend to a lower normal mode. Chen et al. (2019) investigated the two-dimensional structure of a cold eddy in Taiwan and its effect on sound propagation. Their results showed that the eddy structure follows an ellipse; while the largest anomaly occur near the center and at a depth of approximately 400 meters. Its horizontal diameter was 200 km and its vertical diameter was 500 meters. The special model of 2D sound velocity profile for cold eddy was created based on Argo profiles by EOF method. With the feature model, acoustic propagation through both a stationary eddy and a moving eddy was investigated. Results suggest that the presence of the cold eddy could push the convergence zone up to 4 km closer to the source, where it acts as a convex mirror to focus the energy.

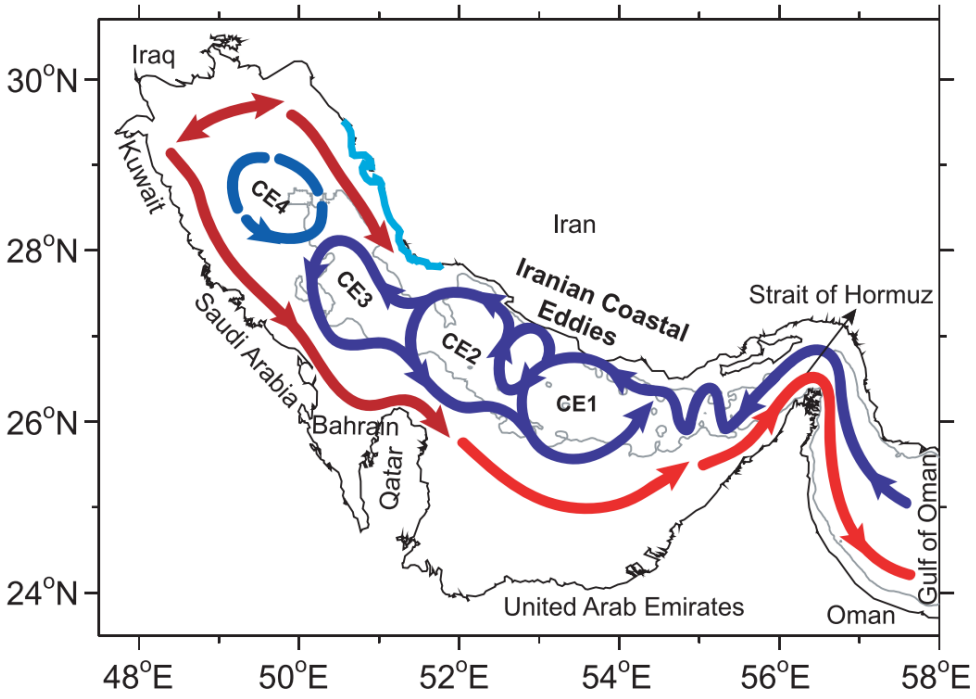


**Figure 1.** Mesoscale eddies in Persian Gulf, CE1, CE2, CE3 and CE4 correspond to the Iranian coastal eddies (Thoppil & Hogan, 2010).

In the field of sound propagation in the southern waters of Iran, Khalilabadi et al. (2023) focused on underwater acoustic modeling in the Gulf of Oman. Additionally, Hosseini et al. (2018) examined the influence of internal tides on sound propagation in the Gulf of Oman. In another study, Khalilabadi (2022) modeled sound propagation in shallow waters. Mahpeykar et al. investigated the effect of cold eddy on acoustic propagation in the Persian Gulf.

## Material and Method

In this research, the algorithm developed by Nencioli et al. (2010) - which is based on rotation of horizontal velocity vector - using MATLAB software to identify eddies (Vector Geometry Algorithm) was used. In terms of appearance, an eddy is defined where the horizontal current vector field revolves around a central point. Based on this characteristic, the algorithm uses four constraints to identify eddies. If these four constraints are met, the existence of an eddy is settled and recorded. These four constraints are as follows:


MARINE REPORTS

1. Along the east-west part of the regular velocity data network, the sign of the velocity component v around a central point must be reversed, and its value increased as it moves away from the center.
2. Along the north-south section, the regular network of velocity data, the sign of the speed component *u* around a central point should be reversed, and its value increased as moving away from the center.
3. The minimum speed value must be set as the center of the eddy.
4. The velocity vector directions should rotate with a constant sense revolving the center of the eddy.

The constraints discussed above need two parameters to be set. One is used for the first, second, and fourth constraints, and the other for the third one. The first parameter called a, determines how many cells in a network around the center point - which have a north-south and east-west velocity - are examined. The second parameter, b, gives the number of cells searched around the reflection point of velocity vectors to determine the minimum velocity. These two parameters define the minimum size of eddies and enable the algorithm to be used for networks with different resolutions. On the other hand, depending on the characteristics and spatial resolution of the data set, the values of these parameters require to be precisely adjusted to optimize the performance of the algorithm (Nencioli et al., 2010).

To validate the algorithm, the velocity vector field maps of some days are randomly chosen and eddies in these maps are visually extracted by experts. According to the studies of Chaigneau et al. state the efficiency of the algorithm can be evaluated by defining two parameters: the success of detection rate (SDR), and the excess of detection rate (EDR). These parameters are defined as follows (Chaigneau et al., 2008):

$$SDR = (N_c / N_{te}) \times 100 \quad (1)$$

$$EDR = (N_{oa} / N_{te}) \times 100 \quad (2)$$

Where $N_{te}$ is the number of real eddies for a certain day, detected by the experts, $N_c$ is the number of eddies for a certain day, detected by the experts and registered by the algorithm, $N_{oa}$ is the number of eddies detected by the algorithm but not recognized as eddies by the experts. Overall, SDR means the accuracy of algorithm detection, and EDR symbolizes the error rate of the algorithm, and the larger and smaller their values, sequentially, the better the performance of the algorithm.

To optimize the algorithm, the velocity components from numerical modeling in the Persian Gulf for seven different days of daily data during a year were randomly selected, and the nodes in them were extracted by experts. Different values of *a* and *b* were reviewed to optimize the algorithm as well. The domain of changes of *a* was between 2 to 10 and the range of changes *b* was between 1 to 10, and a total of 90 various combinations of *a* and *b* were considered to optimize the algorithm. The EDR and SDR diagrams for the various combinations of *a* and *b* are given (Fig. 2). Accordingly, the combination *a=3* and *b=2* has the highest accuracy with a value of around 85% and the lowest error with a value of nearly 12%.


MARINE REPORTS

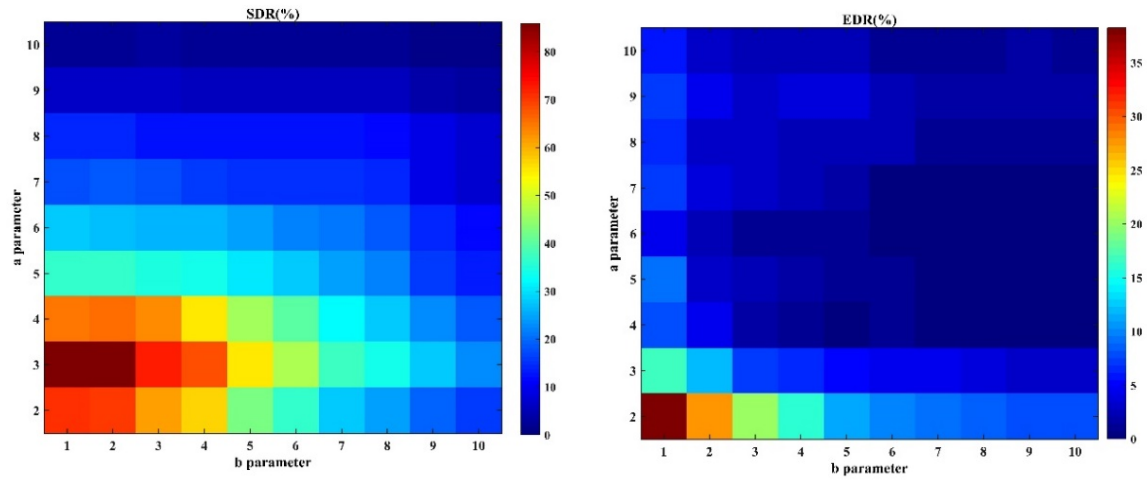


**Figure 2.** Different combinations of *a* and *b* to optimize the algorithm SDR (a), EDR (b).

Table (1) describes the calculation of SDR and EDR for $a = 3$ and $b = 2$. Comparing the values of the table with the results of earlier studies confirms that in the research of Nencioli et al. (2010) for the same algorithm, SDR = 92.9% and EDR = 2.9%. In this research, SDR values beyond 80% were desirable. In the study of Chaigneau et al., the SDR value for the two different methods used was 92.7% and 86.8%; While EDR is 18.7% and 63.3%, sequentially. But, for the differences in the methods as well as the data set used in the studies, it is not possible to directly compare the parameters with each other. For $a = 3$ and $b = 2$, these two parameters provide the best situation for the data of the current study.

**Table 1.** Algorithm validation results for seven chosen days examined by experts

| Day | $N_{te}$ | $N_c$ | $N_{oa}$ | Eddies missed | SDR (%) | EDR (%) |
|---|---|---|---|---|---|---|
| 50 | 36 | 30 | 4 | 6 | 83.3 | 11.1 |
| 100 | 34 | 28 | 2 | 6 | 82.3 | 5.8 |
| 150 | 8 | 7 | 1 | 1 | 87.5 | 12.5 |
| 200 | 10 | 7 | 2 | 3 | 70 | 20 |
| 250 | 12 | 11 | 2 | 1 | 91.6 | 16.6 |
| 300 | 19 | 16 | 1 | 3 | 84.2 | 5.3 |
| 350 | 30 | 28 | 6 | 2 | 93.3 | 20 |
| Total | 149 | 127 | 18 | 22 | 85.2 | 12 |

The propagation of sound at sea depends on the sound speed, and the sound speed is a function of temperature, salinity, and ambient pressure. In the warmer seasons of the year or the warmer part of the day, when the sea surface temperature rises, the speed of sound also increases near the surface. Although the surface of the sea acts as a perfect reflector when it is not wavy, it disperses sound when it is turbulent enough to be comparable in size to the wavelength of sound. Mackenzie introduced the exact relationship between the sound speed in water with a standard error of 0.07 m/s as follows (Mackenzie, 1981):

$$c = 1448.96 + 4.591T - 5.304 \times 10^{-2}T^2 + 2.374 \times 10^{-4}T^3 + 1.340(S - 35) + 1.630 \times 10^{-2}z + 1.675 \times 10^{-7}z^2 - 1.025 \times 10^{-2}T(S - 35) - 7.139 \times 10^{-13}Tz^3 \quad (3)$$


MARINE REPORTS

Where c is the sound speed in m/s, z depth in meters, S salinity in units per thousand (PPT) in the range of 30≤S≤40 and T temperature in degrees Celsius in the range of 0≤T≤30.

BELLHOP is an efficient ray tracing model, which is designed to perform acoustic ray tracing for a given sound speed profile c(z) or a given sound speed field c(r, z), in ocean waveguides with flat or variable absorbing boundaries. Output options include ray coordinates, travel time, amplitude, eigenrays, acoustic pressure or TL (either coherent, incoherent or semi-coherent) (Porter & Bucker, 1987). Input of BELLHOP is environmental file (*.env) to carryout ray tracing and TL, the inputs are given in table (2) that we choose to design *.env, where we have shown the parameters used for modeling the effect of warm eddy on sound propagation.

**Table 2.** Parameters used for acoustic modeling

| Parameter | Value |
|---|---|
| **Source data** | |
| Number of Sources | 1 |
| Source depth | 2, 25, 55 m |
| Source frequency | 2 kHz |
| Source angle | -5 to +5 |
| **Receiver data** | |
| Receiver ranges | 0-154 km |
| Number of receiver ranges | 3001 |
| Receiver depths | 0-82m |
| Number of receiver depths | 135 |
| Number of rays | 1000 |
| Box depths | 82m |
| Box ranges | 154km |
| **Options** | |
| Method of interpolation | ‘QVW’ |
| Type of media | ‘V*’ |
| Type of information required | ‘IB’ |

**Results**

The results of the algorithm are obtained for 25 2-meter layers from the surface to a depth of 50 meters. Fig. (3) gives the eddies identified by the algorithm in the surface layer in early spring. In total, 4308 cyclonic eddies and 2860 anticyclonic eddies were detected in the surface layer and 617 cyclonic eddies and 329 anti-cyclonic eddies in the lowest layer, that is the 50 meters depth. These eddies are positioned on the temperature distribution and have small diameters. In more detail, they form under the influence of local factors, such as topography or wind.

Eddies that have lifetimes of 3 days or more have been extracted to eliminate fluctuations and disturbances in the results of numerical modelling and algorithm detection errors (Dong et al., 2012). Fig. 4 shows the histogram of eddy sizes on the first day of their life and eddy lifetimes at a depth of 10 meters. The values of the positive radius correspond to cyclonic and the negative radius corresponds to the anticyclonic. As can be seen, most eddies have a radius of 5-10 km and are of the cyclonic type. This figure shows that sub-mesoscale eddies are the most abundant and most of them are cyclonic. Histogram of eddy lifetimes also shows that there are more cyclonic with a lifespan of more than 3 days than anticyclonic. The reason for the predominance


MARINE REPORTS

of cyclonic eddies is the general circulation of the Persian Gulf, which is cyclonic. Since eddies usually don't last longer due to wind and will often last due to thermohaline gradients. The main cause of this gradient, which is the inflow of Oman Sea water, causes the development of cyclonic eddies.

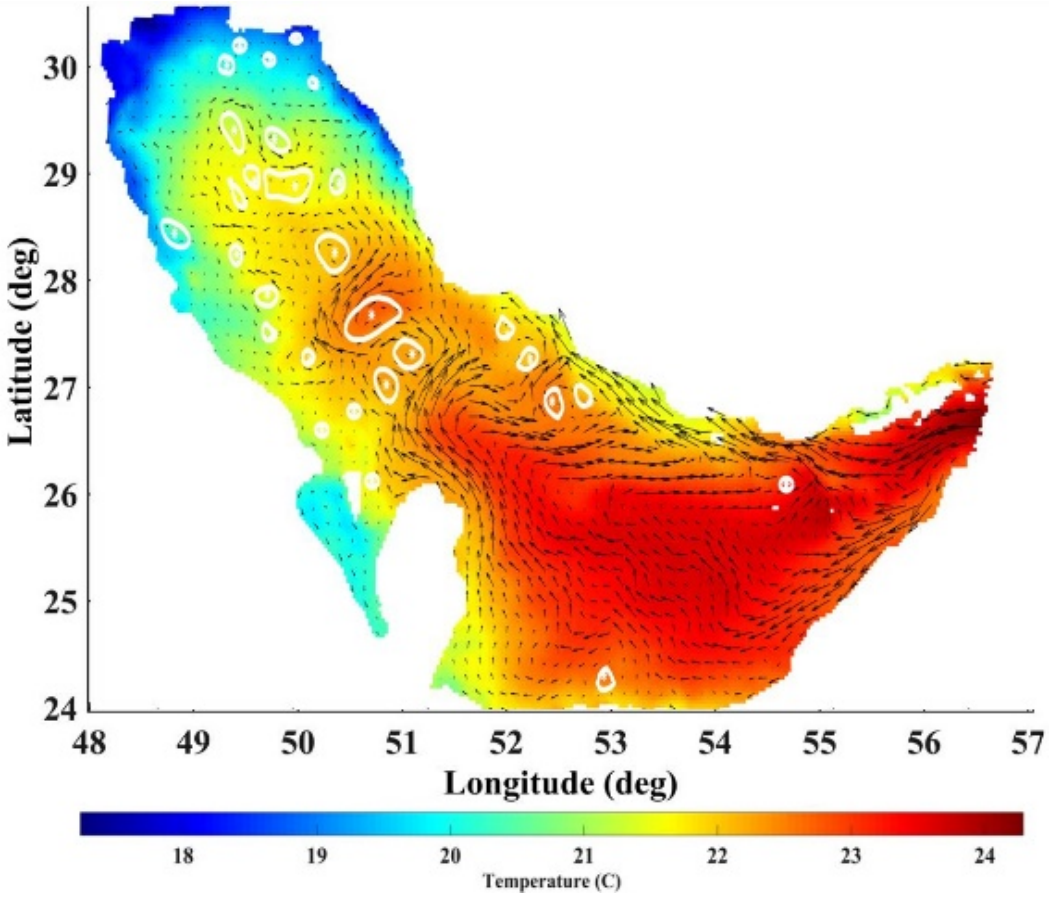


**Figure 3.** Eddies identified by the algorithm

Based on the results of the algorithm tracking, one eddy with a lifespan of 39 days was selected to investigate sound propagation. This eddy has a warm core and its center position, depth and radial changes from the beginning to the end of its duration are shown in Table 3. The minimum and maximum calculated radii for eddy are 4 and 30 km, the lowest of which was recorded on day 39 in the twentieth layer and the highest on the first day and in the twelfth layer. This eddy is generally observed in 25 layers. The sound around this eddy was examined on the 18th day of its life. The position of the eddy center in all layers indicates that the displacement range of the eddy center is 6 cells in the north-south direction and 5 cells in the west-east direction (Fig. 5). According to the dimensions of the cells, this distance is about 16 km in the x direction and 23 km in the y direction (Mahpeykar et al., 2021).


MARINE REPORTS

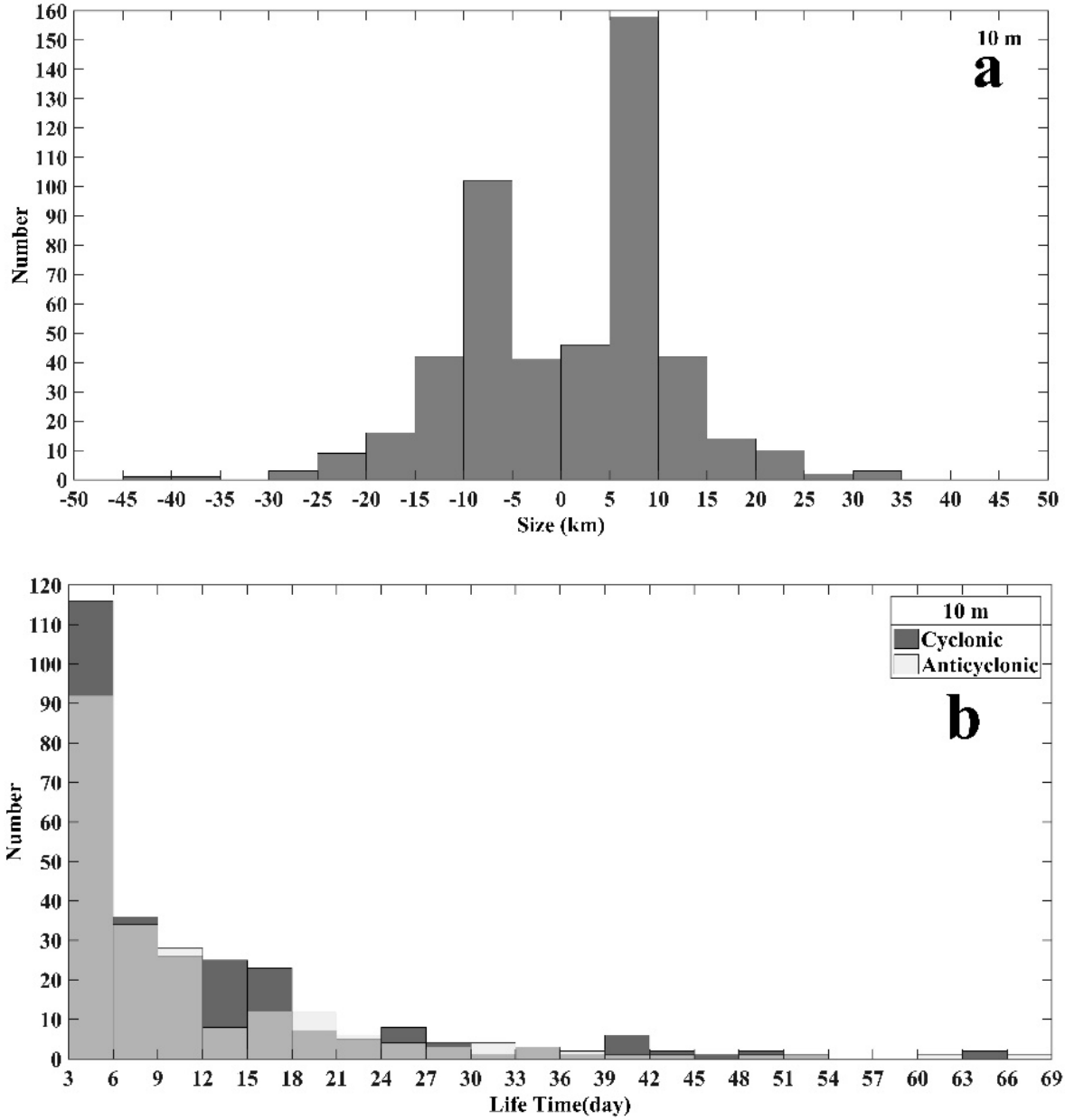


**Figure 4.** Histograms of eddy initial sizes (a) and eddy lifetimes (b). On the upper panel, the left and right sides of "0" on the x-axis denote the anticyclonic and cyclonic eddies, respectively.

Fig. 6 shows the temperature and salinity profiles at the selected point and shows that the eddy is created when the water column has an almost uniform temperature from the surface to the bed but has significant differences in the transverse direction. Since eddy is anticyclonic, it makes sense to expect a warm core, and according to a study by Sun *et al.*, eddy causes convergent motions.

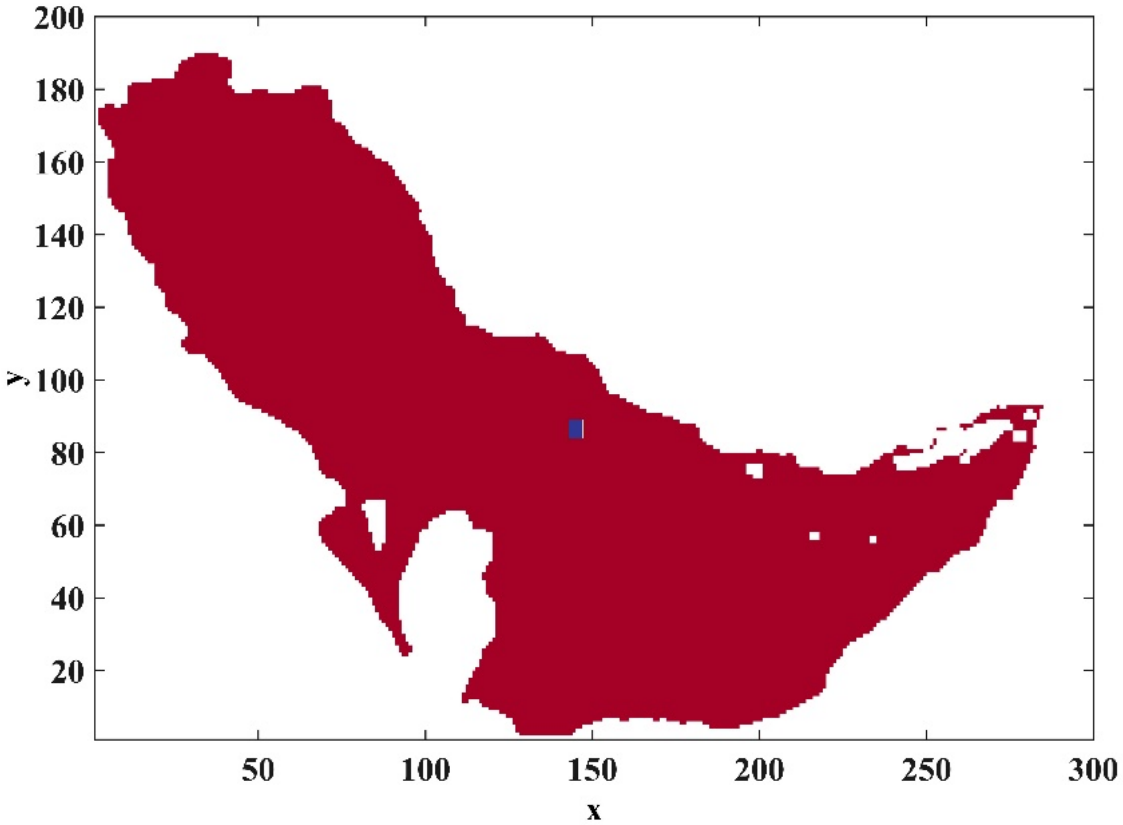


**Figure 5.** Eddy center limited area during lifespan

On the other hand, in winter, due to intense mixing and, consequently, the baroclinic environment, its transverse temperature differences can cause the initial energy to form eddy in this season.

In other words, it can be said that the presence of temperature difference causes the formation of eddy and the development of eddy has increased the temperature difference between the center of eddy and its surroundings, which is considered as a positive-feedback (Sun et al., 2019). In the salinity profile, eddy is not well tolerated due to the lack of salinity difference between the center of the eddy and its surroundings.

To compare the sound propagation as it passed through the eddy, the acoustic profile was calculated at the cross-sectional area passing through the center of the eddy. Then, in the same situation and under the conditions that there was no eddy (in spring), the acoustic profile was calculated (Fig. 7) and the sound propagation was examined under different scenarios. The position of the center of the eddy in the profile of the speed of sound between latitudes 26.6 to 27.4 degrees and to a depth of 40 meters is quite clear. In the absence of eddy, the acoustic profile from the surface to the bed is reduced.


MARINE REPORTS

MARINE REPORTS 3(1) (2024) : 1-20
DOI: 10.5281/zenodo.12335495
marep@scopesscience.com

**Table 3.** The position of the center and the radius of the eddy (in kilometers) during lifespan

| Day→ | 1 | | | 7 | | | 12 | | | 18* | | | 22 | | | 27 | | | 33 | | | 39 | | |
|---|---|---|---|---|---|---|---|---|---|---|---|---|---|---|---|---|---|---|---|---|---|---|---|---|
| Layer↓ Index→ | y | x | r | y | x | r | y | x | r | y | X | r | y | X | R | y | x | r | y | x | r | y | x | r |
| 1 | | | | | | | 85 | 146 | 16 | 85 | 147 | 12 | | | | | | | 85 | 147 | 7 | | | |
| 2 | | | | | | | 85 | 146 | 22 | 84 | 147 | 14 | | | | 86 | 147 | 10 | 85 | 147 | 8 | | | |
| 3 | | | | | | | 85 | 146 | 26 | 84 | 147 | 14 | | | | 86 | 147 | 13 | 85 | 147 | 12 | | | |
| 4 | | | | | | | 85 | 146 | 23 | 84 | 147 | 14 | 85 | 147 | 8 | 86 | 147 | 14 | 85 | 146 | 15 | | | |
| 5 | 87 | 143 | 25 | | | | 86 | 145 | 22 | 84 | 147 | 15 | 85 | 147 | 9 | 86 | 147 | 15 | 85 | 146 | 15 | 86 | 146 | 9 |
| 6 | 87 | 143 | 26 | | | | 86 | 145 | 22 | 84 | 147 | 16 | 85 | 147 | 10 | 86 | 147 | 16 | 85 | 146 | 13 | 86 | 146 | 11 |
| 7 | 87 | 143 | 27 | | | | 86 | 145 | 22 | 85 | 147 | 16 | 85 | 147 | 10 | 87 | 146 | 16 | 86 | 146 | 16 | 86 | 146 | 9 |
| 8 | 87 | 143 | 27 | 87 | 144 | 18 | 86 | 145 | 21 | 85 | 147 | 16 | 85 | 147 | 11 | 87 | 146 | 16 | 86 | 146 | 15 | 86 | 146 | 9 |
| 9 | 87 | 143 | 28 | 87 | 144 | 18 | 86 | 145 | 22 | 85 | 147 | 16 | 85 | 147 | 13 | 87 | 146 | 16 | 86 | 146 | 15 | 86 | 146 | 10 |
| 10 | 87 | 143 | 28 | 87 | 144 | 19 | 86 | 145 | 21 | 86 | 146 | 16 | 85 | 147 | 11 | 87 | 146 | 16 | 86 | 146 | 15 | 86 | 146 | 10 |
| 11 | 87 | 143 | 27 | 87 | 144 | 18 | 86 | 145 | 21 | 86 | 146 | 17 | 85 | 147 | 12 | 87 | 146 | 15 | 86 | 146 | 14 | 86 | 146 | 11 |
| 12 | 87 | 143 | 30 | 87 | 144 | 19 | 86 | 145 | 21 | 86 | 146 | 16 | 85 | 147 | 12 | 87 | 146 | 15 | 86 | 146 | 14 | 86 | 146 | 10 |
| 13 | 87 | 143 | 28 | 87 | 144 | 19 | 86 | 145 | 21 | 86 | 146 | 16 | 85 | 147 | 12 | 87 | 146 | 16 | 86 | 146 | 14 | 86 | 146 | 10 |
| 14 | 87 | 143 | 28 | 87 | 144 | 19 | 86 | 145 | 21 | 86 | 146 | 16 | 85 | 147 | 12 | 87 | 146 | 16 | 86 | 146 | 14 | 86 | 146 | 9 |
| 15 | 87 | 143 | 19 | 87 | 144 | 19 | 86 | 145 | 20 | 86 | 146 | 16 | 85 | 147 | 11 | 87 | 146 | 16 | | | | 86 | 146 | 9 |
| 16 | 87 | 143 | 19 | 87 | 144 | 18 | 86 | 145 | 20 | 86 | 146 | 16 | 85 | 147 | 11 | 87 | 146 | 16 | | | | 86 | 145 | 8 |
| 17 | 87 | 143 | 18 | 87 | 144 | 18 | 86 | 145 | 19 | 86 | 146 | 16 | 85 | 147 | 11 | 87 | 146 | 15 | | | | 86 | 145 | 7 |
| 18 | 87 | 143 | 18 | 87 | 144 | 18 | 86 | 145 | 19 | 86 | 146 | 15 | | | | 87 | 146 | 10 | | | | 86 | 145 | 13 |
| 19 | | | | 87 | 144 | 16 | | | | 86 | 146 | 15 | | | | 87 | 146 | 11 | | | | 86 | 145 | 11 |
| 20 | | | | 87 | 144 | 15 | | | | 86 | 146 | 15 | | | | | | | | | | 86 | 145 | 4 |
| 21 | | | | | | | | | | 86 | 146 | 14 | | | | | | | | | | | | |
| 22 | | | | | | | | | | 86 | 146 | 13 | | | | | | | | | | | | |

MARINE REPORTS 3(1) (2024) : 1-20
DOI: 10.5281/zenodo.12335495
marep@scopesscience.com

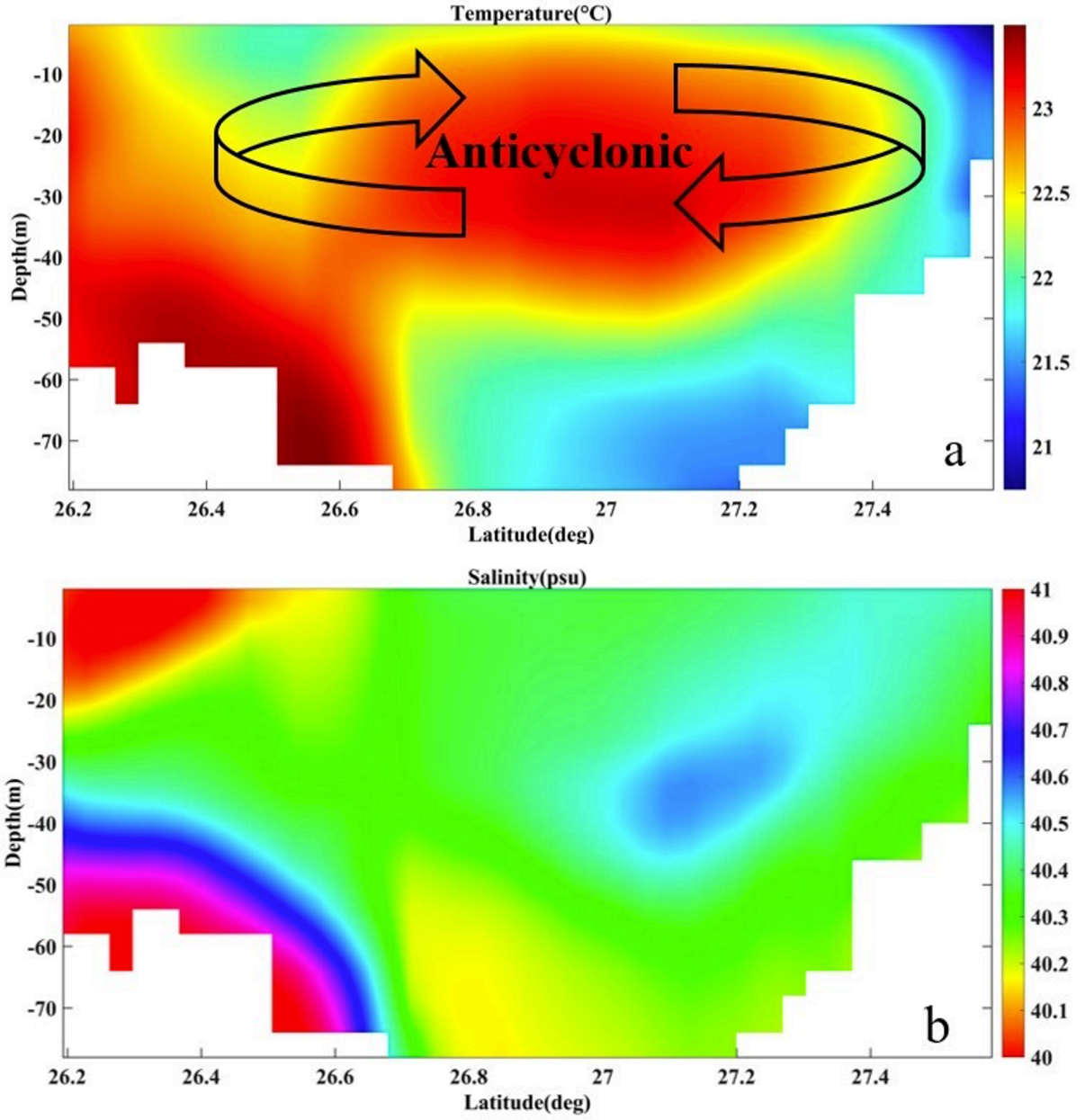


**Figure 2.** Temperature (a) and salinity (b) profiles in the presence of eddy

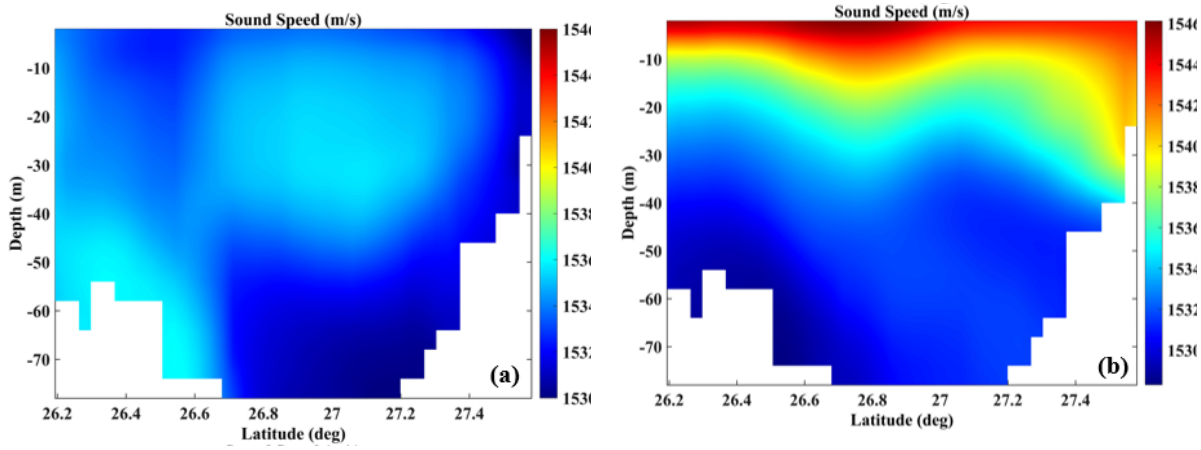


**Figure 3.** Sound speed profile in the presence (a) and absence (b) of eddy

In the case where the source with a frequency of 2 kHz is located at a depth of 2 meters, the TL of sound during the passage of the eddy and in the absence of the eddy, taking into account the topography of the bed, is shown in Fig. 8. In the presence of eddy in the surface layer and a depth of less than 10 meters, a channel appears in which the TL is less, but with increasing depth, the TL increases and in areas close to the center of the eddy, the loss is more severe. Below the central position of the eddy, the sound wave progresses to the point where it disappears when it strikes the wall. In the absence of eddy from the surface to the bed, the sound energy decreases almost uniformly, but in the half-range the propagation is more severe. In addition, there is a sudden increase in loss in the surface layer, which seems to be related to the unevenness of the bed. Comparison of the two figures shows that under these conditions (source depth and wave frequency) TL in the presence of eddy is greater than in the case without eddy, and the greatest amount of TL occurs in the central areas of the eddy and the middle depths.

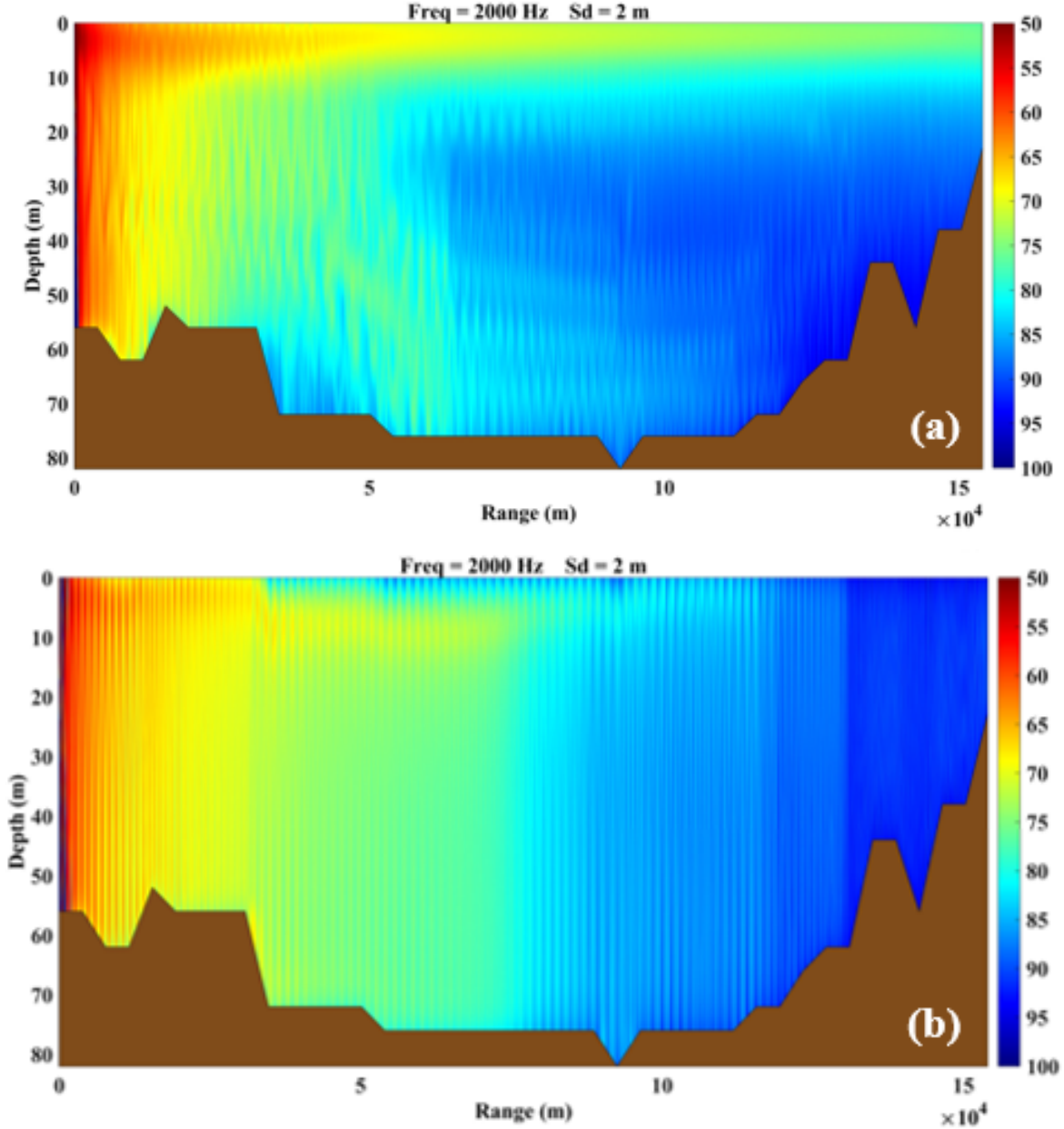


**Figure 4.** Comparison of TLs for environments with (a) and without (b) eddy for the source at a depth of 2 meters


MARINE REPORTS

When the sound source is located at a depth of 25 meters, the TL of sound during the passage of the eddy and in the absence of the eddy is shown in Fig. 9. In these conditions, the TL shows the presence of eddy better, as a channel is created between the central area of the eddy and the surface layer, in which the loss is less, and this channel continues until the end of the eddy range and some sound energy from below the eddy is advancing. In the absence of eddy, except for the surface area where the loss is severe, at depths of more than 20 m the loss is increased almost uniformly throughout the propagation range. The depth of the surface layer has changed in proportion to the topographic changes, so that with increasing depth, the depth of this layer has increased. A comparison of the two figures shows that under these conditions, the greatest loss occurred in the surface layer without the presence of eddy.

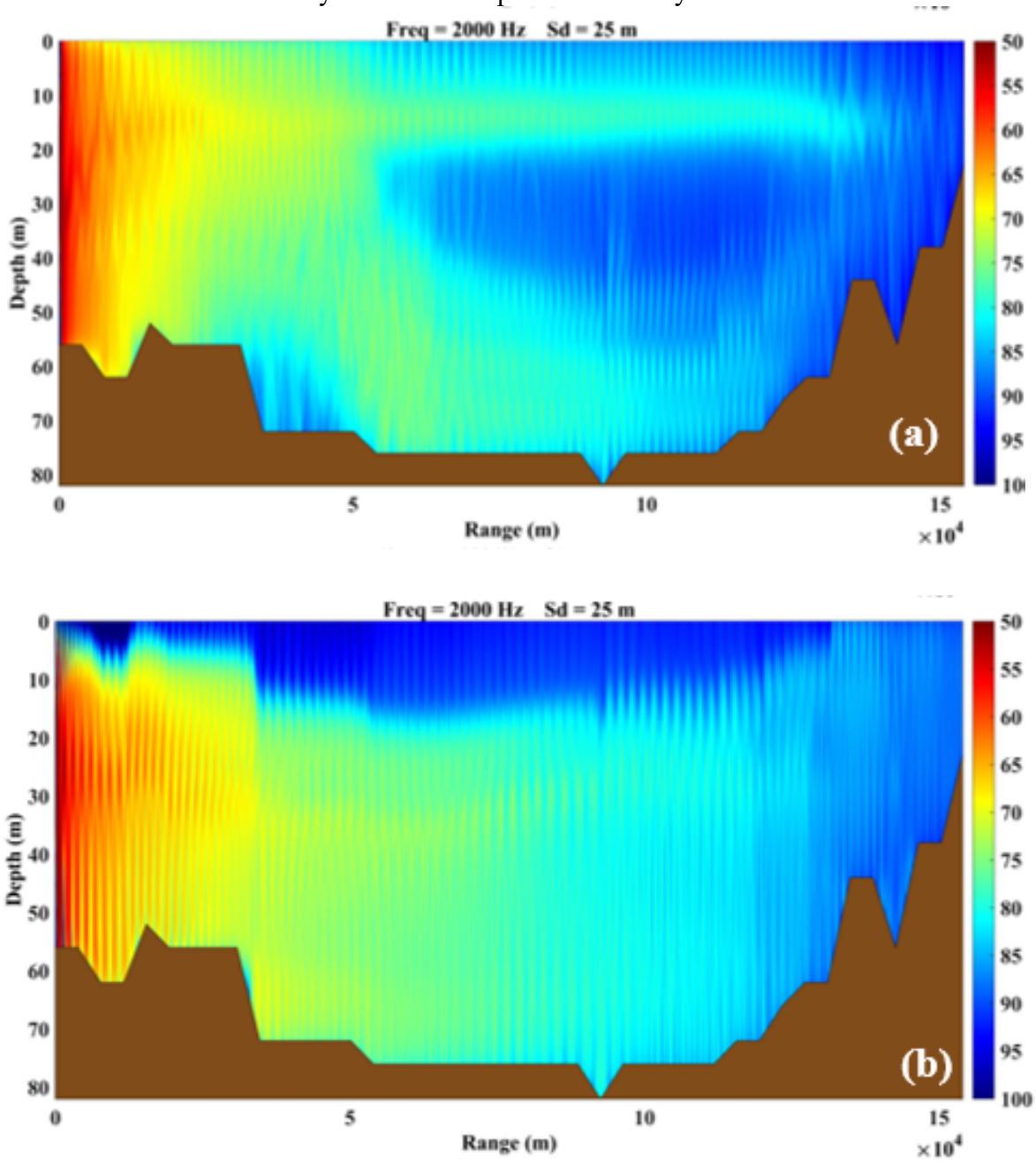


**Figure 5.** Comparison of TLs for environments with (a) and without (b) eddy for the source at a depth of 25 meters


MARINE REPORTS

When the sound source is located at a depth of 55 meters, the TL during the passage of the eddy and in the absence of the eddy is shown in Fig. 10. In the presence of eddy, the loss below the eddy range is similar to the previous state, but the channel on the eddy that was created in the previous state has disappeared and sound energy can only be emitted from under the eddy. In the absence of eddy, the amount of loss in the surface layer is less than in the previous case, but in the first ten kilometres of propagation and sound energy has not reached the surface layer.

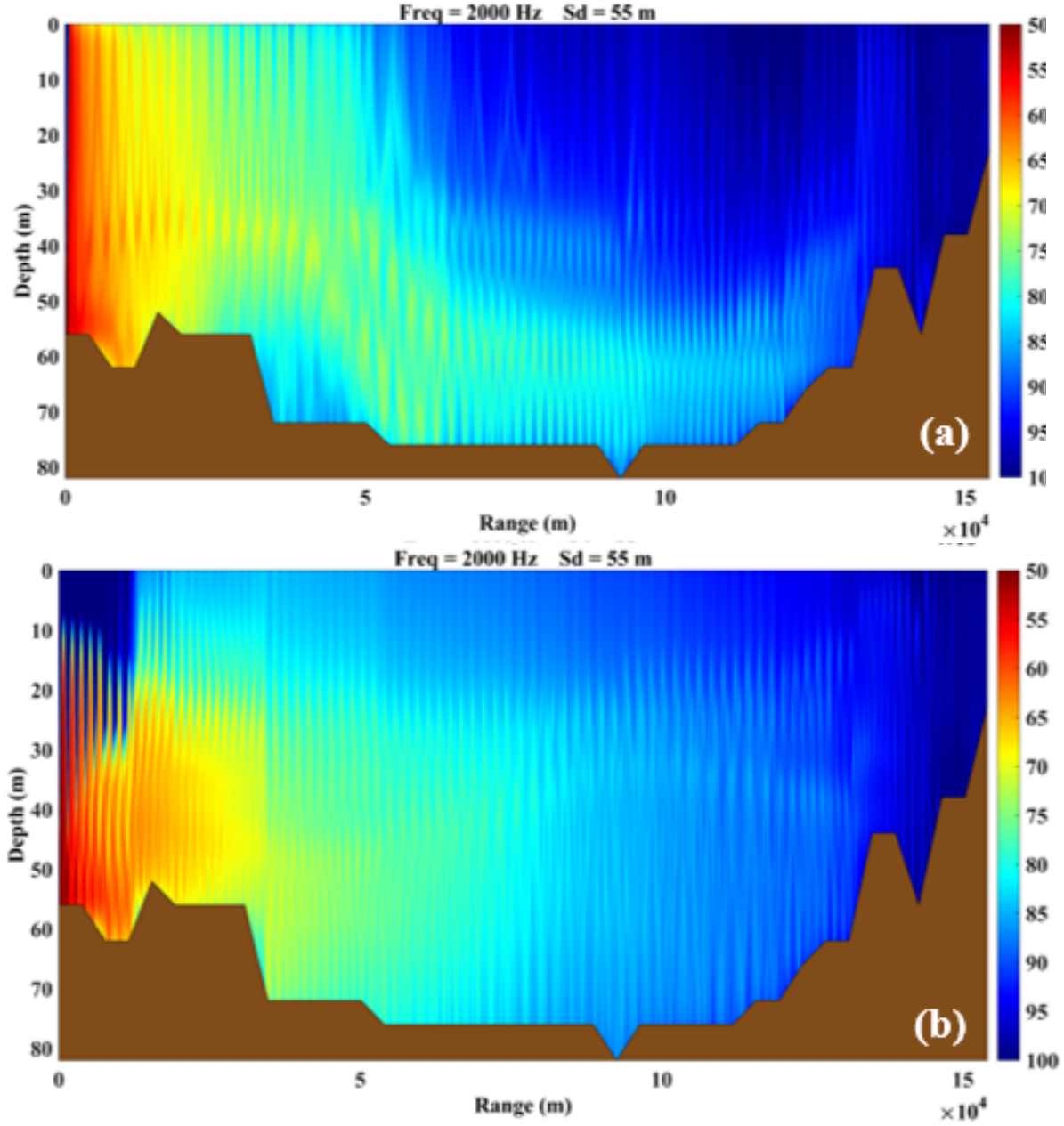


**Figure 6.** Comparison of TLs for environments with (a) and without (b) eddy for the source at a depth of 55 meters

Fig. 11 shows the TL for the sound source and receivers at depths of 2, 25, and 55 m in the presence and absence of eddy. When the source and receiver are located at a depth of 2 meters, the TL is less in the presence of eddy, which was due to the creation of a channel on top of the eddy, but when the source and receiver are located at a depth of 25 meters, between 50 and 130 km, the presence of eddy causes The rate of loss has increased in this range and at other intervals the loss is almost similar to the absence of eddy. In the position of the source and receiver at a


MARINE REPORTS

depth of 55 meters, because the effect of eddy at this depth is not very noticeable, there is no difference between the presence and absence of eddy.

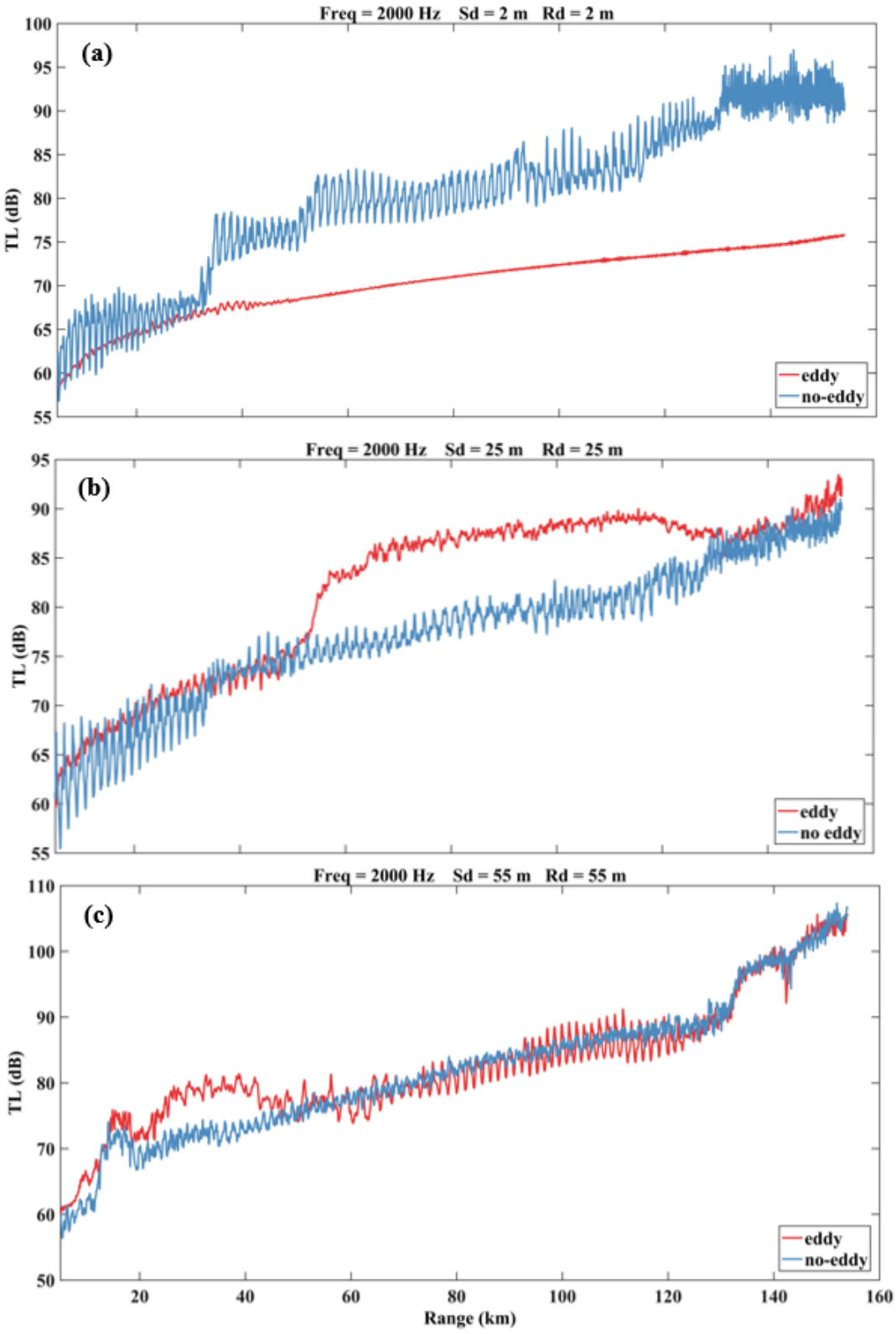


**Figure 7.** Comparison of TLs for environments with/without eddy for the source and receivers at a depth of 2 (a), 25 (b) and 55 (c) meters

Here we examine the propagation of sound in three dimensions in the presence and absence of eddy. The frequency used in this case is 2 kHz and the TL has been investigated for placing the source at three different depths. These experiments were performed considering the topography of the bed and as shown in Fig. 13, the deepest area of this part of the Gulf is located in the northwest-southeast direction and its depth is more than 70 meters. There is a steep coastal slope on the coast of Iran and a relatively gentle slope on the opposite side, which leads to the Arabian coast.

Fig. 14 shows the TL at three different depths, and what is clearly seen in these figures is that the TL in the northwest-southeast direction is less than in other directions, which shows this dependence on topography; but in other directions the situation will be examined. At a depth of two meters in the northeastern direction, the amount of loss in the presence of eddy is more than the absence of eddy, but in the southwestern direction, the situation is the opposite, i.e. in the presence of eddy, the amount of loss is less than in the absence of eddy. At a depth of 25 meters, the situation is similar to a depth of two meters, with the difference that in the northeast direction there is a relative reduction in loss, and this exists for both cases, although in the absence of eddy more sharp fluctuations in loss in the radial direction is observed.

At a depth of 50 meters, the greatest difference is seen between the two states, where in the absence of eddy, the amount of loss in the northeast direction reaches its lowest point among all states. Due to the fact that there is a weak layering in the absence of eddy under these conditions and the temperature of the underlying layers is lower than the surface layer, it seems that sound propagation at a depth of 50 meters is easier because at low temperatures the speed of sound is lower. At this depth and in the presence of eddy, the amount of dissipation at discrete angles shows a relative decrease, and at those angles the propagation range reaches a greater radius. Also, the fluctuations of loss at this depth and in the presence of eddy are more severe than at higher depths, especially with increasing distance from the source.

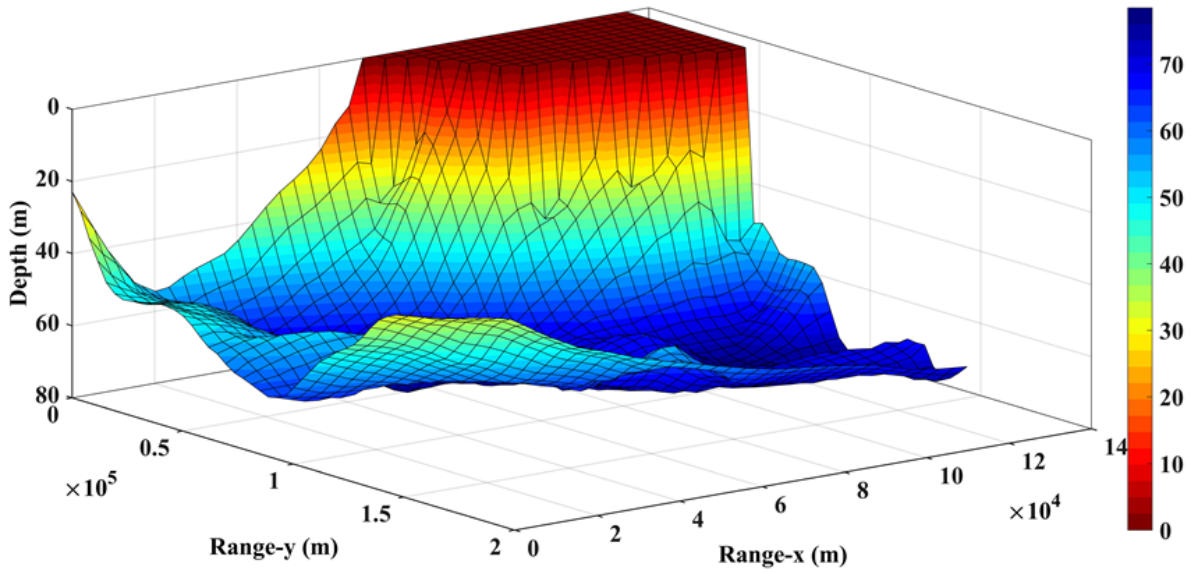


**Figure 8.** Bed topography in the area of the desired eddy


MARINE REPORTS

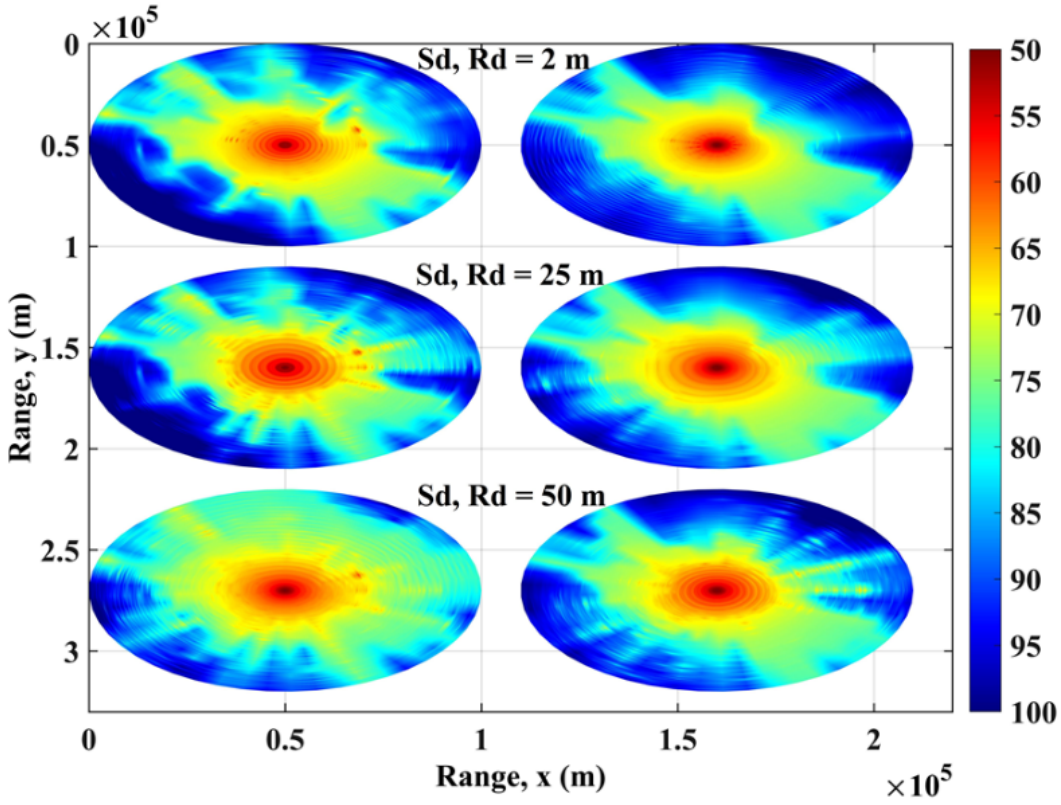


**Figure 9.** Three-dimensional transmission loss at different depths in the presence (right) and absence of eddy (left)

**Discussion**

Due to the mixing of water in winter, the sound when passing through the eddy from the surface to the bed does not show much difference; but the behavior of sound can vary depending on the depth of the source and the distance of the source from the center of the eddy. The greatest difference in depth is observed when the horizontal temperature and salinity gradient is greater between the center and around the eddy. Due to the fact that the largest radius of these eddy is in the middle layers, the highest horizontal gradients of temperature and salinity occur in these layers. When the source is on the surface, the loss in the surface layer is minimal, but when the source is located in the middle or near the bed, the role of eddy in the sound loss becomes more prominent. Under these conditions, the loss is greater than without the eddy, and the greater the sound speed difference between the center and around of the eddy, the greater the TL.

Studies to date have examined the effect of eddy on sound propagation in deep water, while the behavior of sound is different in shallow water and is highly sensitive to temperature and salinity inequality (Katsnelson et al., 2012). However, in the study of Xiao et al. (2019) it has been shown that warm eddy has a divergence effect on acoustic energy. Examination of signal fluctuations shows that the presence of warm eddy causes less delay in the received signal than in the case without eddy. Also, received signals occur twice with a slight time difference. The effect of warm eddy divergence on the signal also seems to be noticeable. In the surface layer, only the second series of signals are received, and thus it can be concluded that the second series of signals is related to the rays that have passed through the top of the eddy and the signals passing from the bottom of the eddy have not reached the surface layer. But in the middle and deep depths, both series of signals are received. Also, according to the sound speed profile (Fig.


MARINE REPORTS

7), the lower layer, close to the bed, has a lower sound speed, and therefore the signal passing through this area reaches the end of the propagation band faster.

## Conclusion

In this study, the effect of warm eddy on sound propagation was investigated and as it was observed, in winter the vertical structure of water is mixed and the temperature and salinity in the Persian Gulf from the surface to the bed show slight changes. Under these conditions, the formation of eddy causes the horizontal temperature gradients in the vertical column to be clearly visible, and therefore their presence can affect the changes in sound velocity in the horizontal direction. From another point of view, the salinity and temperature changes around the eddy in the horizontal direction are such that the temperature or salinity will increase or decrease as it approaches the center of the eddy, and this trend will be reversed as it moves away from the center of the eddy. The minimum desired values (temperature or salinity) will occur in the center of the eddy. The propagation of sound in the seas has a lot to do with the physical properties of the marine environment. So far many studies have been done to study the behavior of sound under the influence of different structures. Eddies, as one of the most important oceanic and marine structures that can occur on a small to large scale, also affect the speed profile of sound. In this study, for the first time, the pattern of sound propagation in the Persian Gulf due to eddy (as a shallow structure) has been investigated. The results showed that the presence of eddy in winter increases the TL compared to the state without eddy and warm eddy causes divergence of sound energy. Also, the depth of the source is very important in the TL and the warm eddy causes less time delay in the received signal.

## Ethical approval

Not applicable.

## Informed consent

Not available.

## Data availability statement

The authors declare that data can be provided by corresponding author upon reasonable request.

## Conflicts of interest

There is no conflict of interests for publishing this study.

## Funding organizations

No funding available for this study.

## Contribution of authors

Omid Mahpeykar: Conceptualization, Data curation, Formal analysis
Amir Ashtari Larki: Supervisor, Resources, Validation, Visualization, Review, Editing
Mohammad Akbarinansab: Investigation, Methodology, Software

**References**

Chaigneau, A., Gizolme, A., & Grados, C. (2008). Mesoscale eddies off Peru in altimeter records: identification algorithms and eddy spatio-temporal patterns, *Progress in Oceanography, 79*(2-4), 106-119. https://doi.org/10.1016/j.pocean.2008.10.013

Chen, C., Gao, Y., Yan, F., Jin, T., & Zhou, Z. (2019). Delving into the Two-Dimensional Structure of a Cold Eddy East of Taiwan and Its Impact on Acoustic Propagation. *Acoustics Australia, 47*, 185–193. https://doi.org/10.1007/s40857-019-00160-7

Dong, C., Lin, X., Liu, Y., Nencioli, F., Chao, Y., Guan, Y., Chen, D., Dickey, T., & McWilliams, J. C. (2012). Three dimensional oceanic eddy analysis in the Southern California Bight from a numerical product. *Journal of Geophysical Research, 117*, 1-17. https://doi.org/10.1029/2011JC007354

Dong, C., Nencioli, F., Liu, Y., & McWilliams, J. C. (2011). An automated approach to detect oceanic eddies from satellite remotely sensed sea surface temperature data. IEEE Geoscience and Remote Sensing Letters, *8*(6), 1055-1059. https://doi.org/10.1109/LGRS.2011.2155029

Fu, L. L., Chelton, D. B., Le Traon, P. Y., & Morrow, R. (2010). Eddy dynamics from satellite altimetry. *Oceanography, 23*, 14–25. https://doi.org/10.5670/oceanog.2010.02

Hosseini, S. H., Akbarinasab, M., & Khalilabadi, M. R. (2018). Numerical simulation of the effect internal tide on the propagation sound in the Oman sea. *Journal of the Earth and Space Physics, 44*(1), 215-225. https://doi.org/10.22059/JESPHYS.2018.221834.1006867

Jia-xun, L., Ren, Z., Chen-zhao, L., & Hong-Jun, F. (2012). Modeling of ocean mesoscale eddy and its application in the underwater acoustic propagation. *Marine Science Bulletin, 14*(1), 1-15. http://hdl.handle.net/1834/5830

Katsnelson, B., Petnikov, V., & Lynch, J. (2012). *Fundamentals of shallow water Acoustics,* Springer, *540p*. https://doi.org/10.1007/978-1-4419-9777-7

Khalilabadi, M. R. (2022). 2D modeling of wave propagation in shallow water by the method of characteristics. *Archives of Acoustics, 47*(3), 407-412. https://doi.org/10.24425/aoa.2022.142014

Khalilabadi, M., Shahmirzaei, H., & DaneshMehr, S. (2023). Underwater acoustic modeling in the Gulf of Oman. *Journal of Acoustical Engineering Society of Iran, 10*(2), 21-34. http://joasi.ir/article-1-252-en.html

Li, J. X., Zhang, R., & Chen, Y. D. (2011). Ocean mesoscale eddy modeling and its application in studying the effect on underwater acoustic propagation. *Marine Science Bulletin, 30*, 37–46. http://hdl.handle.net/1834/14814

Mackenzie, K. V. (1981). Nine-term equation for sound speed in the oceans. *The Journal of the Acoustical Society of America, 70*, 807-808. https://doi.org/10.1121/1.386920

Mahpeykar, O., Ashtari Larki, A., & Akbarinasab, M. (2021). Numerical Modelling and Automatic Detection of submesoscale eddies in Persian Gulf Using aVector Geometry Algorithm. *Journal of the Earth and Space Physics, 47*(1), 109-125. https://doi.org/10.22059/JESPHYS.2021.307109.1007237

Mahpeykar, O., Ashtari Larki, A., & Akbarinasab, M. (2022), The Effect of Cold Eddy on Acoustic Propagation (Case Study: Eddy in the Persian Gulf). *Archives of Acoustics, 47*(3), 413-423. https://doi.org/10.24425/aoa.2022.142015

Nencioli, F., Dong, C., Dickey, T., Washburn, L., & McWillams, C. J. (2010). A Vector Geometry–Based Eddy Detection Algorithm and Its Application to a High-Resolution Numerical Model Product and High-Frequency Radar Surface Velocities in the Southern California Bight. *Journal of Atmospheric and Oceanic Technology, 27*, 564-579. https://doi.org/10.1175/2009JTECHO725.1

Porter, M. B., & Bucker, H. P. (1987). Gaussian beam tracing for computing ocean acoustic fields. *The Journal of the Acoustical Society of America, 82*(4), 1349-1359. https://doi.org/10.1121/1.395269

Pous, S., Lazre, P., & Carton, X. (2015). A model of the general circulation in the Persian Gulf and in the Strait of Hormuz: Intraseasonal to interannual variability. *Continental Shelf Research, 94*, 55–70. https://doi.org/10.1016/j.csr.2014.12.008

Reynolds, R. M. (1993). Physical oceanography of the Gulf, Strait of Hormuz and the Gulf of Oman—Results from the Mt. Mitchell expedition. *Marine Pollution Bulletin, 27,* 35–59. https://doi.org/10.1016/0025-326X(93)90007-7

Sun, W., Dong, C., Tan, W., & He, Y. (2019). Statistical Characteristics of Cyclonic Warm-Core Eddies and Anticyclonic Cold-Core Eddies in the North Pacific Based on Remote Sensing Data. *Remote Sensing, 11*(208), 1-22. https://doi.org/10.3390/rs11020208

Thoppil, P. G., & Hogan, P. J. (2010). A modeling study of circulation and eddies in the Persian Gulf. *Journal of Physical Oceanography, 40,* 2122–2134. https://doi.org/10.1175/2010JPO4227.1

Xiao, Y., Li, Z., Li, J., Liu, J., & Sabra, K. G. (2019). Influence of warm eddies on sound propagation in the Gulf of Mexico. *Chinese Physical Society and IOP Publishing Ltd*, *28*(5), 054301-1-11. https://doi.org/10.1088/1674-1056/28/5/054301

Zhang, Z., Wang, W., & Qiu, B. (2014). Oceanic mass transport by mesoscale eddies. *Science 18, 345*(6194), 322-333. https://doi.org/10.1126/science.1252418